

BRITISH ACOUSTICAL SOCIETY

71/01

Scattering Phenomena in Acoustics

26 February 1971

A COMPARISON OF GEOMETRICAL FEATURES AS ACOUSTIC SCATTERERS WITHIN A FLUID

A Freedman

This paper first summarises the principal acoustic scattering mechanisms which apply to smooth, rigid scattering bodies immersed in an isotropic, fluid medium. Concentrating on backscattering from bodies of simple, generally convex or plane shape, the features giving rise to echo components are examined and formulae and curves showing the size of these components are culled from the literature. Finally, an attempt is made to categorise the echo producing features in order of their importance.

The mechanism of direct backscattering from rigid surfaces having dimensions and radii of curvature large compared with the wavelength has been described in Refs 1 and 2 and is illustrated schematically in Fig 1, where it is assumed the transmitter and receiver are distant from the scattering body. Echo components, termed Image Pulses, are produced at each range where there is a discontinuity in $A(r)$ or in one of its derivatives of any order, J , $A(r)$ being the projected area towards the transmitter of all those parts of the scatterer within range r . The shadow regions are deemed to make no contributions to this mechanism.

Taking into account only the lowest order of derivative in which there is a contributing discontinuity, the magnitude of an Image Pulse may be expressed as

$$|E| = C F(\theta, \phi) L_1 (kL_2)^N, \quad (1)$$

where C is a normalising constant, $F(\theta, \phi)$ is a function of the direction in which the scatterer is insonified, L_1 and L_2 are quantities with dimensions of length, and N is equal to $-(J - 1)$. Thus, the higher the order of derivative in which a discontinuity occurs, the smaller the corresponding Image Pulse is likely to be. For any one discontinuity, $F(\theta, \phi)$ may cover a considerable range of values as the insonification direction is varied.

Fig 2 shows the derivation of the Image Pulse echo structure for axial insonification of two simple bodies, a spherical cap and a cone. The two echo components from the spherical cap and that from the base of the cone are each associated with a discontinuity in $dA(r)/dr$, while that from the cone apex is associated with a discontinuity in $d^2A(r)/dr^2$.

The variation of Image Pulse magnitudes with direction of insonification is brought out in Fig 3 in the curves for a cylinder; these curves were calculated by Dumsiger, in Ref 3, who showed reasonable experimental supporting evidence for them.

The Creeping or so-called Franz waves are initiated at the geometrical shadow boundary and circulate repeatedly round a smooth body with exponential decay, radiation being continually sprayed off tangentially (Fig 4). (See, for example, Refs 4 to 6). The phase velocity of Franz waves is a little lower than that of free field waves and approaches the latter value at high frequencies. Echo components are produced after each circulation round the body and the magnitude of the first of these for a sphere or cylinder can be expressed approximately as

$$|E| \approx L_1 (kL_2)^{\frac{1}{2}} \exp[-M (kL_2)^{\frac{1}{2}}] \quad (2)$$

where L_1 and L_2 have the previous meanings and M is non-dimensional.

For a rigid sphere, Deppermann and Franz's curves (Ref 5) portraying the magnitude of the first creeping wave component relative to that of the "geometrically reflected component" (i.e., the Image Pulse) show the Creeping Wave mechanism to be relatively insignificant for backscattering from spheres at least a few wavelengths in diameter, but to be of increasing relative importance with increasing bi-static angle.

For rigid bodies whose dimensions are at least a few wavelengths, an attempt is made in Fig 5 to place the contributions to backscattering from various geometrical features in order of relative importance. Plane waves are deemed incident from the left. In Fig 5, the effect of $F(\theta, \phi)$ on Image Pulse magnitudes is ignored, the features being placed vertically in order of decreasing N . Fractional values of N arise from results calculated by Dumsiger using the methods of Ref 7. It is implied that the higher up an item appears in Fig 5, the larger the echo contribution it is likely to cause. A tri-plane and a corner are included because, although they involve multiple scattering, their echoes can be expressed in the form of Eq 1. The following order of importance of features emerges. 1. Surface normal to wavefront; 2. Line where surface locally normal to wavefront; 3. Line normal to wavefront beginning or terminating surface at an angle to the wavefront. Also, near point of domed surface; 4. Smoothly rounded near or far limit of plane or curved surface. 5. Cone apex or corner of flat surface. Rather doubtful, equirange shadow boundary on continuous surface. 6. Near or far point of shadow boundary on discontinuous surface.

Creeping Wave contributions are also shown in Fig 5 and, although for these N has the value $\frac{1}{2}$, their contributions are shown in a lower position because of the exponential attenuation term.

References

1. A Freedman, "A mechanism of acoustic echo formation". *Acustica* 12, 10, 1962.
2. A Freedman, "The high frequency echo structure of some simple body shapes". *Acustica* 12, 61, 1962.

3. A D Dunsiger, "High frequency acoustic echoes received from simple geometric shapes with possible application to target recognition". *J Sound Vib* 13, 323, 1970.
4. W Franz and K Deppermann, "Theorie der Beugung am Zylinder unter Berücksichtigung der Kriechwelle". *Ann Phys* 10, 361, 1952.
5. K Deppermann and W Franz, "Theorie der Beugung an der Kugel unter Berücksichtigung der Kriechwelle". *Ann Phys* 14, 253, 1954.
6. H Überall, R D Doolittle and J V McNicholas, "Use of sound pulses for a study of circumferential waves". *J Acoust Soc Am* 39, 564, 1966.
7. J W Crispin Jr, R P Goodrich and K M Siegel, "A theoretical method for the calculation of radar cross sections of aircraft and missiles". University of Michigan Radiation Lab Rep 1959.

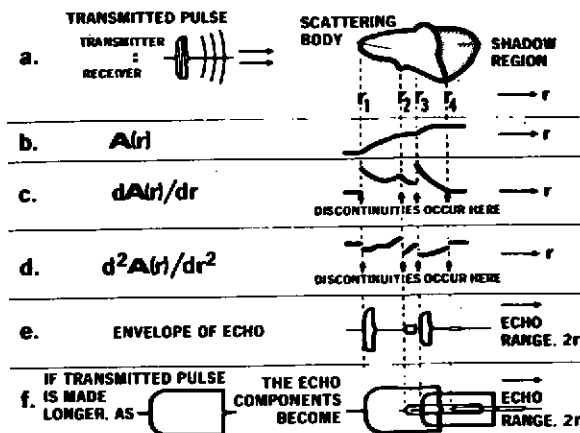
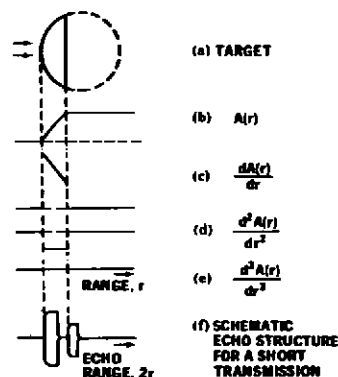


Fig 1
Image
Pulse
mechanism

SPHERICAL CAP



CONE

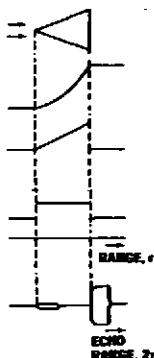


Fig 2
Echo structure
of spherical
cap and cone

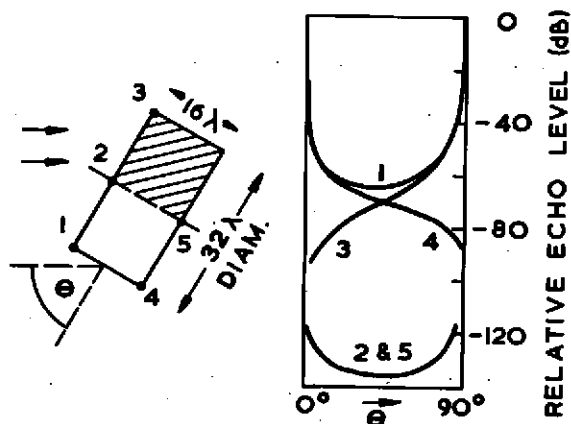


Fig 3 Magnitude of echo components for cylinder. After Dumsiger.

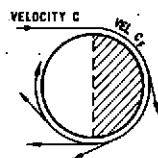


Fig 4 Creeping (or Franz) wave mechanism.




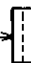
















N	ECHO COMPONENTS OF FORM $E \propto L_1 \times (kL_2)^N$				ECHO COMPONENTS OF FORM $E \propto L_1 \times (kL_2)^{1/2}$ $\propto \exp \left[N \ln (kL_2)^{1/2} \right]$
1	 PLANE SURFACE	 TRI-PLANE	 CORNER		
$1/2$	 CYLINDER	 CONE			
0	 RECTANGULAR PLATE	 SPHERICAL CAP	 CONE	 SPHERE	 SPHEROID
$-1/2$	 CIRCULAR PLATE	 CYLINDER	 CONE		
-1	 RECTANGULAR PLATE	 CONE	 SPHERE	 SPHEROID	
	DOUBTFUL				
-2	 CYLINDER	 CONE			SPHERE AND CYLINDER 

Fig 5 Relative importance of echo components from different features. (Largest components at top, smallest at bottom).